

## Mutations in *SLC26A1* Cause Nephrolithiasis

Heon Yung Gee,<sup>1,2,10</sup> Ikhyun Jun,<sup>1,3,10</sup> Daniela A. Braun,<sup>2</sup> Jennifer A. Lawson,<sup>2</sup> Jan Halbritter,<sup>2,4</sup> Shirlee Shril,<sup>2</sup> Caleb P. Nelson,<sup>5</sup> Weizhen Tan,<sup>2</sup> Deborah Stein,<sup>2</sup> Ari J. Wassner,<sup>6</sup> Michael A. Ferguson,<sup>2</sup> Zoran Gucev,<sup>7</sup> John A. Sayer,<sup>8</sup> Danko Milosevic,<sup>9</sup> Michelle Baum,<sup>2</sup> Velibor Tasic,<sup>7</sup> Min Goo Lee,<sup>1,\*</sup> and Friedhelm Hildebrandt<sup>2,\*</sup>

Nephrolithiasis, a condition in which urinary supersaturation leads to stone formation in the urinary system, affects about 5%–10% of individuals worldwide at some point in their lifetime and results in significant medical costs and morbidity. To date, mutations in more than 30 genes have been described as being associated with nephrolithiasis, and these mutations explain about 15% of kidney stone cases, suggesting that additional nephrolithiasis-associated genes remain to be discovered. To identify additional genes whose mutations are linked to nephrolithiasis, we performed targeted next-generation sequencing of 18 hypothesized candidate genes in 348 unrelated individuals with kidney stones. We detected biallelic mutations in *SLC26A1* (solute carrier family 26 member 1) in two unrelated individuals with calcium oxalate kidney stones. We show by immunofluorescence, immunoblotting, and glycosylation analysis that the variant protein mimicking p.Thr185Met has defects in protein folding or trafficking. In addition, by measuring anion exchange activity of *SLC26A1*, we demonstrate that all the identified mutations in *SLC26A1* result in decreased transporter activity. Our data identify *SLC26A1* mutations as causing a recessive Mendelian form of nephrolithiasis.

Nephrolithiasis (MIM: 167030) is a major health problem given that it affects up to 10% of the population in Western countries. Its prevalence has significantly increased among children over the last decades.<sup>1,2</sup> This leads to significant medical cost due to expensive surgical interventions, progression to chronic kidney disease, and additional morbidity from renal colic and secondary urinary tract infection.<sup>3</sup> The formation of kidney stones is multifactorial, resulting from an interaction of environmental, dietary, and genetic factors. Nephrolithiasis is genetically heterogeneous, and mutations in at least 30 genes have been linked to this disorder.<sup>4,5</sup> We recently demonstrated in a cohort of 166 adults and 106 children with nephrolithiasis or nephrocalcinosis that a monogenic cause can be detected in the surprisingly high percentage of 11.4% of adult cases and 20.8% of childhood-onset cases.<sup>6</sup> In a follow-up study, we detected causative mutations in 1 of 30 linked genes in 16.7% of 143 individuals who manifested with nephrolithiasis or nephrocalcinosis before 18 years of age.<sup>7</sup> Both studies thus demonstrated a high percentage of individuals with a monogenic mutation associated with kidney stone formation. However, genetic factors have been suggested to account for nearly 50% of nephrolithiasis cases,<sup>8,9</sup> indicating that additional nephrolithiasis-associated genes remain to be discovered.

To identify additional genes mutated in nephrolithiasis, we generated a list of 18 hypothetical candidate genes and performed exon amplification with consecutive next-gen-

eration sequencing in a multicenter cohort of 348 individuals with nephrolithiasis or isolated nephrocalcinosis.<sup>10</sup> The cohorts were previously described, and consisted of 201 children and 147 adults who had at least one urinary stone or nephrocalcinosis.<sup>6,7</sup> For exclusion of known genetic causes of nephrolithiasis, 30 genes previously linked to nephrolithiasis were screened by exon sequencing in these individuals, but no causative mutations were detected. Written informed consent was obtained from all individuals enrolled in this study, and approval for human subject research was obtained from the institutional review boards at the Boston Children's Hospital. The candidate genes screened in this study are listed in [Table S1](#). We designed 210 target-specific primer pairs for coding exons and the adjacent splice site of 18 genes. Amplicon sizes were chosen to range from 250 to 300 base pairs. We achieved a median sequencing coverage of 198× per individual and 192× per amplicon. Only 9/350 (2.5%) individuals had a median coverage below 20.

In an individual of Macedonian descent (A3054-21) who is from non-consanguineous parents and clinically presented with acute renal failure due to bilateral obstructive calculi, nephrocalcinosis, and bilateral ureteropelvic junction obstruction (UPJO), we detected two compound-heterozygous mutations in *SLC26A1* (solute carrier family 26 member 1 [GenBank: NM\_022042.3] [MIM: 610130]) ([Table 1](#), [Figure 1](#), and [Figure S1](#)). This individual had acute renal failure due to ureteral obstruction with calculi at the

<sup>1</sup>Department of Pharmacology, Brain Korea 21 PLUS Project for Medical Sciences, Yonsei University College of Medicine, Seoul 03722, Republic of Korea;

<sup>2</sup>Division of Nephrology, Department of Medicine, Boston Children's Hospital and Harvard Medical School, Boston, MA 02115, USA; <sup>3</sup>The Institute of Vision Research, Department of Ophthalmology, Yonsei University College of Medicine, Seoul 03722, Korea; <sup>4</sup>Division of Endocrinology and Nephrology, Department of Internal Medicine, University Clinic Leipzig, Leipzig 04103, Germany; <sup>5</sup>Divisions of Urology and General Pediatrics, Department of Medicine, Boston Children's Hospital and Harvard Medical School, Boston, MA 02115, USA; <sup>6</sup>Division of Endocrinology, Department of Medicine, Boston Children's Hospital and Harvard Medical School, Boston, MA 02115, USA; <sup>7</sup>Medical Faculty Skopje, University Children's Hospital, Skopje 1000, Macedonia;

<sup>8</sup>Institute of Genetic Medicine, International Centre for Life, Newcastle University, Central Parkway, Newcastle upon Tyne NE1 3BZ, UK; <sup>9</sup>Department of Pediatric Nephrology, Dialysis, and Transplantation, Clinical Hospital Center Zagreb, University of Zagreb Medical School, Zagreb 10000, Croatia

<sup>10</sup>These authors contributed equally to this work

\*Correspondence: [mlee@yuhs.ac](mailto:mlee@yuhs.ac) (M.G.L.), [friedhelm.hildebrandt@childrens.harvard.edu](mailto:friedhelm.hildebrandt@childrens.harvard.edu) (F.H.)

<http://dx.doi.org/10.1016/j.ajhg.2016.03.026>

© 2016 American Society of Human Genetics.

**Table 1. Recessive SLC26A1 Mutations Detected in Individuals with Nephrolithiasis**

Individual	Sex	Ethnic Origin	Parental Consanguinity	Nucleotide Change <sup>a</sup>	Amino Acid Change	Exon (Zygoty, Segregation)	Amino Acid Sequence Conservation <sup>b</sup>	PP2 <sup>c</sup>	MT <sup>d</sup>	Frequencies in the EVS Database <sup>d</sup>	Frequencies in the dbSNP Database <sup>d</sup>	Frequencies in the ExAC Database <sup>d</sup>	Age of Onset	Stone Analysis
A3054-21	M	Macedonian	no	c.554C>T	p.Thr185Met	2 (het, M)	<i>D. rerio</i>	0.996	DC	AA/GA/GG = 0/5/6,480	rs139024319 (MAF = 0.0006)	26/104,290 (no hom)	5 yr	CaOx
				c.1073C>T	p.Ser358Leu	3 (het, P)	<i>D. rerio</i>	1.000	DC	AA/GA/GG = 0/4/6,386	rs148832260 (MAF = 0.0002)	10/24,944 (no hom)		
B641-12 (MA-1015)	M	European American	yes	c.166G>A	p.Ala56Thr	2 (HOM, ND)	<i>M. musculus</i>	0.523	SNP	TT/CT/CC = 0/5/6,487	rs142573758 (MAF = 0.0002)	59/112,248 (no hom)	ND	CaOx

Abbreviations are as follows: CaOx, calcium oxalate; DC, disease causing; het, heterozygous in affected individual; HOM, homozygous in affected individual; M, heterozygous mutation identified in mother; MAF, minor-allele frequency; MI, male; MT, MutationTaster; NA, not applicable; ND, no data or DNA available; P, heterozygous mutation identified in father; PP2, PolyPhen-2 prediction score HumVar; yr, years.  
<sup>a</sup>cDNA mutations are numbered according to the human cDNA reference sequence for SLC26A1 (GenBank: NM\_022042.3); +1 corresponds to the A of ATG translation initiation codon.  
<sup>b</sup>Amino acid residue is continually conserved throughout evolution including the species as indicated.  
<sup>c</sup>polyPhen-2 prediction score HumVar ranges from 0 to 1.0; 0 = benign, 1.0 = probably damaging. See [Web Resources](#).  
<sup>d</sup>See [Web Resources](#).

age of five. He had recurrent episodes of renal colic due to calcium oxalate nephrolithiasis and hypocalcemia and underwent surgery for UPJO. The analysis of 24 hr urine showed that this individual also had hyperoxaluria; otherwise, urine and blood chemistries were normal (Table S2). The two compound heterozygous missense mutations (c.554C>T, p.Thr185Met and c.1073C>T, p.Ser358Leu) in SLC26A1 are reported as SNPs in the dbSNP database; however, their minor allele frequencies are below 0.0006 and they never occurred in a homozygous state (Table 1). The amino acid residues affected by two missense mutations were conserved throughout evolution down to *Danio rerio* (Table 1 and Figure 1). Because this individual had UPJO, we therefore performed whole-exome sequencing (WES) and examined variants in genes associated with congenital anomalies of the kidney and urinary tract (CAKUT) or UPJO. However, we could not detect any additional pathogenic variants in these genes. In addition, we examined genomic structural abnormality by using WES data, but no structural variation was detected.

In a European-American boy (B641-12) who had nephrolithiasis and was born to consanguineous parents, we detected a homozygous missense mutation in SLC26A1 (Table 1, Figure 1, and Figure S1). The paternal grandfather of this individual also had nephrolithiasis. A kidney stone was initially found in this individual during a computerized tomography scan, which was performed for the evaluation of abdominal pain. In a 24 hr urine test, oxalate was within normal range (Table S2). Renal function of this individual was normal. The detected missense mutation (c.166G>A, p.Ala56Thr) is reported as a SNP in the dbSNP database; however, its minor allele frequency is 0.0002 and it never occurred in a homozygous state (Table 1). Murine SLC26A1 has Ala at the position corresponding to amino acid position 56 of human SLC26A1, whereas the protein from *Xenopus tropicalis* or *Danio rerio* has Val, which is also chemically related as a non-charged non-polar residue (Table 1 and Figure 1).

SLC26A1 (also known as SAT1) was cloned as a sulfate transporter from liver.<sup>11</sup> It was subsequently characterized as an anion exchanger that transports anions by mediating electroneutral sulfate-oxalate, sulfate-bicarbonate, or oxalate-bicarbonate exchange.<sup>12,13</sup> The *Slc26a1*<sup>-/-</sup> mice exhibit hyposulfatemia, hypersulfaturia, calcium oxalate urolithiasis, and nephrocalcinosis in the setting of hyperoxalemia and hyperoxaluria.<sup>14</sup> *Slc26a1*<sup>-/-</sup> mice also show infiltration of leukocytes around renal cortical vessels, suggestive of UPJO.<sup>14</sup> In this regard, it is of note that one of the individuals with SLC26A1 mutations (A3054-21) had UPJO, which could be based on a pathogenesis similar to the one described in the murine model. In addition, *Slc26a1*<sup>-/-</sup> mice show enhanced drug-induced liver toxicity, which might reflect reduced availability of intracellular sulfate ion for drug conjugation reactions.<sup>14</sup> These findings demonstrate that, in mammals, SLC26A1 plays a critical role in oxalate and sulfate homeostasis, which is thought to be associated with kidney stone disease.

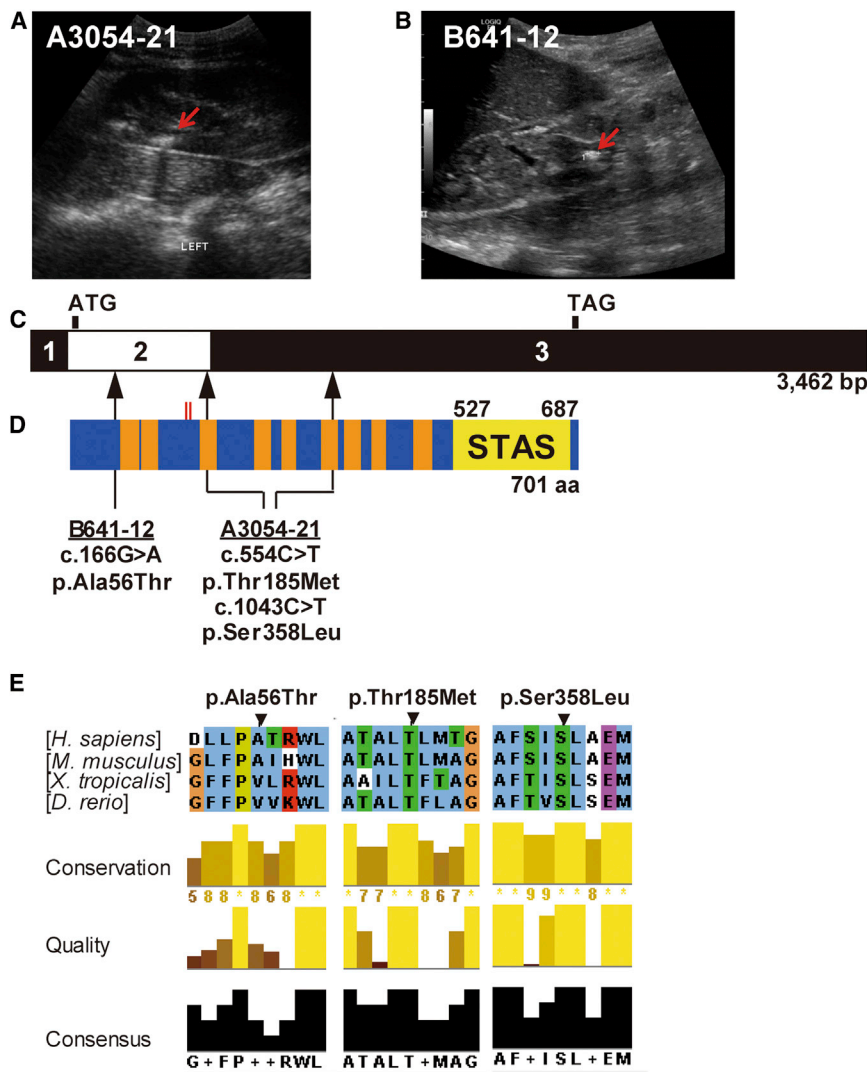


**Figure 1. Identification of Recessive *SLC26A1* Mutations in Two Individuals with Nephrolithiasis**

(A and B) Renal sonography of individuals A3054-21 (A) and B641-12 (B) reveals kidney stones.

(C) Exon structure of human *SLC26A1* cDNA. *SLC26A1* contains three exons. Positions of the start codon (ATG) and stop codon (TAG) are indicated.

(D) Domain structure of *SLC26A1*. The transmembrane (orange) and sulfate transporter and AntiSigma factor antagonist (STAS) domains are depicted by colored bars, in relation to encoding exon position. *SLC26A1* has two N-linked glycosylation sites (amino acid positions 158 and 163, red lines). Three homozygous or compound-heterozygous *SLC26A1* mutations detected in two families with nephrolithiasis are shown. Family numbers (underlined), mutations, and predicted translational changes are indicated (see Table 1).

(E) A partial protein alignment of *SLC26A1* shows evolutionary conservation of the identified missense changes.

negative intercalated cells of collecting ducts in the medulla (Figures 2A and 2B). *SLC26A1* also localizes to cytoplasm and basolateral membranes of the ileum and colon (Figure 2C and 2D).

To evaluate the impact of the identified human mutations on *SLC26A1* function, we performed immunofluorescence in HEK293T cells upon overexpression of wild-type (WT) and mutant *SLC26A1*s. A mouse *Slc26a1* clone was purchased from Open Biosystems (clone accession no. BC025824), and mutant clones of *Slc26a1* were generated by PCR-based site-directed mutagenesis. The WT protein and the variant protein harboring p.Ala56Thr localized to plasma membranes (Figure 2E), whereas the p.Thr190Met variant (which corresponds to p.Thr185Met in human protein) failed to reach the plasma membrane and was trapped in the endoplasmic reticulum (ER) as shown by colocalization with an ER marker, BiP (Figure 2E). The *SLC26A1* variant harboring p.Ser363Leu, which corresponds to p.Ser358Leu in human protein, reached the cell surface; however, a significant portion of protein was trapped in the ER, suggesting a processing defect (Figure 2E). The protein amounts of WT and variant *SLC26A1*s were analyzed in HEK293T and also in PANC-1 cells (Figure 3). Because PANC-1 cells derived from pancreatic ducts retain epithelial properties and do not have endogenous *SLC26A1*, they constitute a suitable model for studying protein processing through transfection of plasmids encoding WT and variant *SLC26A1*s (Figure 3). *SLC26A1* undergoes the Golgi-mediated complex-glycosylation (band

However, to date, the contribution of genetic variants in *SLC26A1* to nephrolithiasis in human is unknown. Dawson et al. examined *SLC26A1* in 13 individuals with recurrent calcium oxalate urolithiasis,<sup>15</sup> but they were unable to detect any biallelic mutations in *SLC26A1*. The c.1667A>G, p.Gln556Arg variant, which was found in 6 out of 13 individuals examined, including one homozygous individual, is a known SNP (rs3706622), and its allele frequency is 0.6737 (26,773 homozygotes out of 79,535 individuals are reported in the Exome Aggregation Consortium [ExAC] Browser), suggesting that this SNP is probably benign, rather than disease causing.

The *SLC26A1* transporter is known to localize at the basolateral membrane of renal proximal tubular epithelial cells and enterocytes, as well as at the sinusoidal membrane of hepatocytes.<sup>14,16,17</sup> We confirmed by immunofluorescence the localization of *SLC26A1* in the rat kidney and intestine (Figure 2). We show that *SLC26A1* is present in the basolateral membrane of peanut lectin-positive proximal tubules in the renal cortex and basolaterally in the AQP2-positive principle cells, as well as the AQP2-

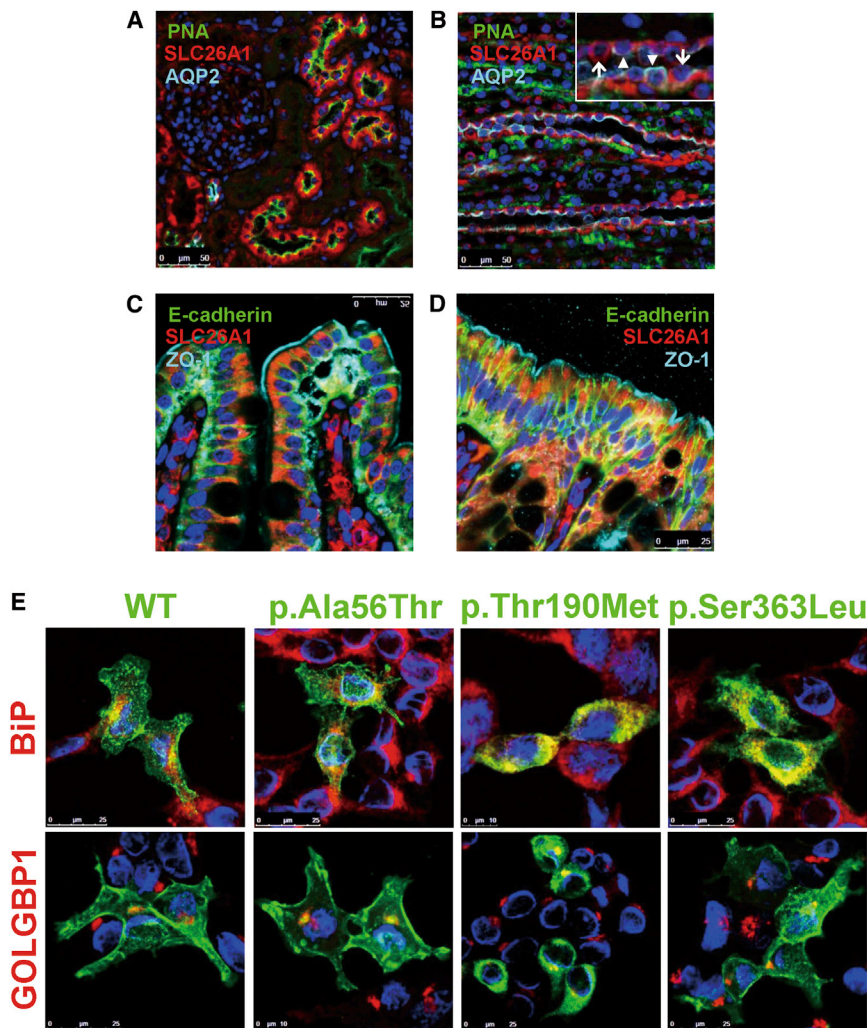


**Figure 2. Localization of SLC26A1 in the Kidney and Intestine and the Effects of SLC26A1 Mutation on Subcellular Localization of SLC26A1**

(A and B) Localization of SLC26A1 in the renal cortex (A) and medulla (B). Rat kidney sections were immunostained with fluorescein isothiocyanate-labeled peanut lectin (PNA) for proximal tubules, anti-SLC26A1 (rabbit polyclonal, Novus Biological, 1:200), and anti-aquaporin 2 (AQP2, mouse monoclonal, Santa Cruz Biotechnology, 1:100) for principal cells of collecting ducts antibodies. In the renal cortex, SLC26A1 (red) mainly localized to proximal tubules, which were marked green by PNA (A). In the medulla, SLC26A1 (red) was present in collecting duct principle cells (arrowheads), which were marked apically blue-green by AQP2, but also in intercalated cells (arrows), which were not marked by AQP2 (2 $\times$  for inset) (B). (C and D) Localization of SLC26A1 in the ileum (C) and colon (D). Intestines from rat were immunostained with anti-E-cadherin (mouse monoclonal, BD Transduction Laboratories, 1:100), anti-SLC26A1, and anti-Zona Occludens-1 (ZO-1, goat polyclonal, Santa Cruz Biotechnology, 1:100) antibodies. E-cadherin and ZO-1 mark adherens and tight junctions, respectively. (E) Immunofluorescence of WT and variant proteins of SLC26A1 in HEK293T cells. HEK293T cells were transfected with N-terminally Myc-tagged WT *Slc26a1* or mutant clones. Cells were fixed and permeabilized with methanol and immunostained with anti-Myc (mouse monoclonal, Cell Signaling Technology, 1:200), anti-BiP (rabbit polyclonal, Abcam, 1:100), and anti-GOLGBP1 (rabbit polyclonal, Sigma, 1:100) antibodies. BiP and GOLGBP1 mark the endoplasmic reticulum and Golgi apparatus, respectively.

C) after an initial core-glycosylation at the ER (band B). In general, the Golgi-glycosylated forms of SLC26A1 are present at the cell surface. When we examined the protein amounts of variant proteins, we found them significantly reduced, as compared to WT proteins (Figures 3A and 3D). SLC26A1 p.Thr190Met in particular was not processed to the fully glycosylated form (Figures 3A and 3D), which suggests that the p.Thr190Met protein is degraded via the ER-associated protein degradation (ERAD) pathway and is consistent with the finding that the p.Thr190Met protein was not observed in the plasma membrane (Figure 2E).

To confirm whether the lower band of SLC26A1 in immunoblotting truly represented the ER form, we treated the protein samples of WT SLC26A1 and the p.Thr190Met variant with endoglycosidase H (Endo H) and peptide-N-glycosidase F (PNGase F) (Figures 3B and 3E). The band size of Endo-H-treated WT sample did not change (band C), whereas the band size of the PNGase-F-treated sample decreased to that of the p.Thr190Met variant pro-

tein. On the other hand, the band size of the Endo-H-treated p.Thr190Met variant protein (band B) decreased to that of PNGase-F-treated WT or p.Thr190Met SLC26A1 (band A). The Endo-H-sensitive digestion of the p.Thr190Met protein suggests that this variant protein exists as an ER form (band B). We performed real-time PCR experiments to determine whether the reduced amounts of variant proteins were due to a reduced number of transcripts or to poor protein stability. We found that the number of transcripts of *Slc26a1* was not significantly different in cells transfected with WT and mutant plasmids (Figure S2), indicating that mRNA of WT *Slc26a1* and mRNAs harboring mutations are not different at the transcription level. These results also indicate that reduced amounts of the p.Ser363Leu variant protein is associated with deficient protein stability.

To verify functional abnormalities of SLC26A1 variant proteins, we measured the anion transporting activity of SLC26A1 by monitoring intracellular pH (pH<sub>i</sub>) in HEK293T cells after transfection with *Slc26a1* plasmids

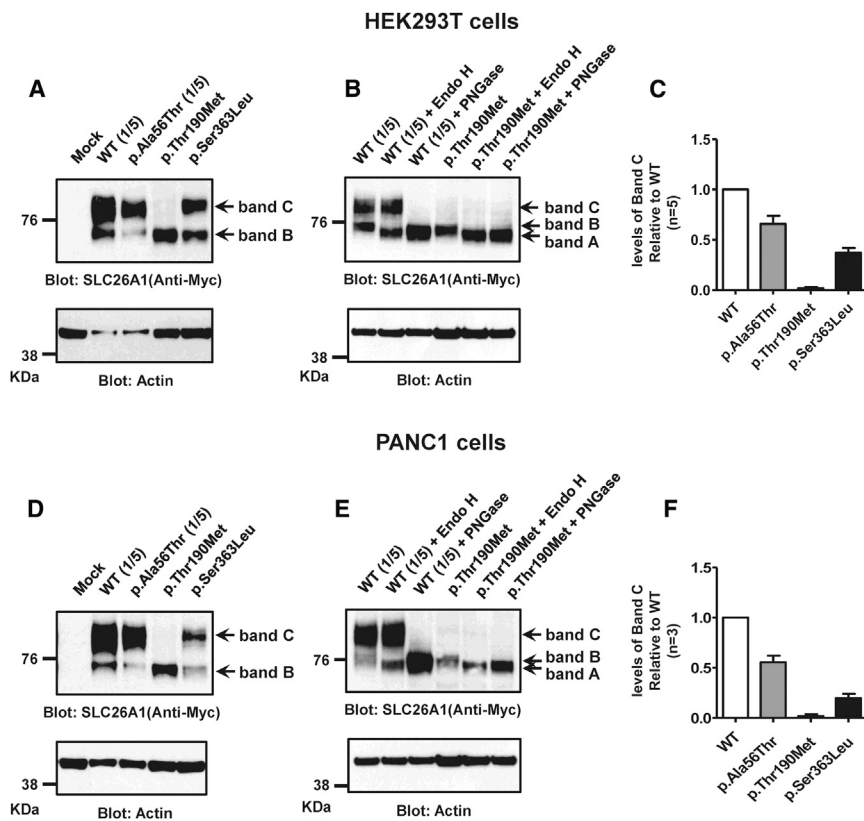


**Figure 3. Immunoblotting and Real-Time PCR Assay of Wild-Type and Variant SLC26A1 Proteins**

(A) HEK293T cells were transfected with *Slc26a1* WT and mutant plasmids, and immunoblotting assays of SLC26A1 were performed. Cells were harvested, and the protein samples were separated by SDS-polyacrylamid gel electrophoresis. The separated proteins were transferred to a nitrocellulose membrane and blotted with appropriate primary and secondary antibodies. Anti-Myc (mouse monoclonal, Santa Cruz Biotechnology, 1:1000) antibody was used as primary antibody, and anti-Mouse IgG (HRP) (Thermo Scientific) antibody was used as secondary antibody. Protein bands were detected by enhanced chemiluminescence (Amersham Biosciences). Due to higher protein amounts of the WT SLC26A1 and p.Ala56Thr variant than of the p.Thr190Met or p.Ser363Leu variants, one-fifth of protein sample was used for WT SLC26A1 and the p.Ala56Thr variant.

(B) Samples from cells expressing WT- or p.Thr190Met-SLC26A1 were digested with endoglycosidase H (Endo H, New England Biolabs) and peptide N-glycosidase F (PNGase F), according to the manufacturer's instructions. In the WT protein, complex glycosylated form, band C was not shifted after treatment of Endo H and was shifted to band A after treatment of

PNGase F. In the p.Thr190Met variant, core glycosylated form, band B is dominant and was shifted to band A after treatment with Endo H. The p.Thr190Met variant is degraded by the ER-associated degradation (ERAD) pathway.

(C) Relative protein amounts of band C of SLC26A1 variants in HEK293T cells. All variants showed lower protein amounts than the WT protein.

(D) Immunoblotting assays of SLC26A1 in PANC-1 cells. The results were comparable with those in HEK293T cells.

(E) Treatment of glycosidase in PANC-1 cells showed a similar effect to that seen in HEK293T cells.

(F) Relative protein amounts of band C of SLC26A1 variants in PANC-1 cells.

(Figure 4). We measured  $pH_i$  with a pH-sensitive fluorescent probe, 2',7'-Bis(2-carboxyethyl)-5(6)-carboxyfluorescein acetoxymethyl ester (BCECF-AM), as described previously.<sup>18</sup> Previous studies have revealed that SLC26A1 can transport chloride, bicarbonate, oxalate, and sulfate.<sup>12,19,20</sup> Although SLC26A1 also has  $HCO_3^-$ -oxalate exchange activities (Figure S3), we instead analyzed SLC26A1-mediated  $SO_4^{2-}$ - $HCO_3^-$  exchange activities because of a technical advantage allowing us to observe more robust  $pH_i$  changes in these activities (Figure 4). We first loaded HEK293T cells with  $HCO_3^-$  by using endogenous  $Cl_i$ - $HCO_3^-$  exchange activities. Then, we analyzed the initial rate of  $pH_i$  reduction due to  $HCO_3^-$ - $SO_4^{2-}$  exchange activities after challenging the cells with 25 mM  $SO_4^{2-}$ . As shown in Figures 4A and 4B, cells expressing SLC26A1, but not mock-transfected cells, showed a strong  $HCO_3^-$ - $SO_4^{2-}$  exchange activity. Subsequently, we measured the transport activities of SLC26A1 variant proteins in the same manner. Compared to WT SLC26A1, all the variants showed decreased  $HCO_3^-$ - $SO_4^{2-}$  exchange activities (Figures 4B–4E), especially the folding defect mutant, p.Thr190Met, for which activity almost vanished

(Figure 4D). The summaries of difference and slope of intracellular pH are given in Figure 4F.

Here, using a candidate gene approach, we demonstrate that mutations in *SLC26A1* cause an autosomal-recessive form of calcium oxalate nephrolithiasis. Our functional studies indicate that all the identified mutations in *SLC26A1* lead to decreased transporter activity. Hyperoxalemia in *Slc26a1*<sup>-/-</sup> mice was most likely caused by reduced intestinal secretion of oxalate, based on reduced oxalate transport in basolateral membrane vesicles from the distal ileum, cecum, and proximal colon, as well as decreased cecal oxalate content. Hyperoxalemia led to hyperoxaluria and calcium oxalate nephrolithiasis. Similarly, reduced intestinal secretion of oxalate, which resulted from decreased transporter activity, probably led to calcium oxalate stones in individuals with *SLC26A1* mutations. *Slc26a1*<sup>-/-</sup> mice have increased liver sensitivity to acetaminophen.<sup>14</sup> Administration of acetaminophen led to a 4-fold increase in serum alanine transaminase levels and extensive liver necrosis in *Slc26a1*<sup>-/-</sup> mice.<sup>14</sup> Therefore, it will be of high clinical relevance to determine whether individuals with biallelic mutations in *SLC26A1* also exhibit drug-induced

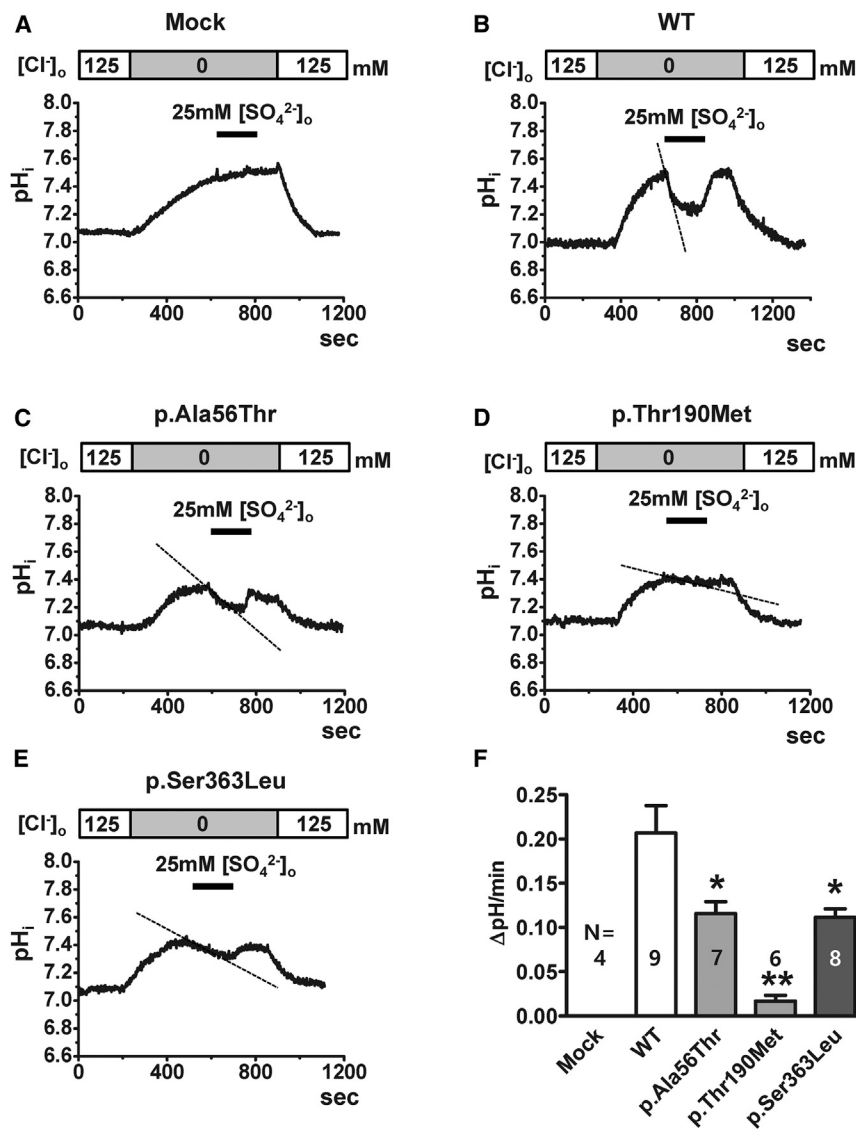


**Figure 4. Measurement of  $\text{HCO}_3^-$ -sulfate exchange activity**

Measurements of  $\text{pH}_i$  in transfected HEK293T cells were performed with the pH-sensitive fluorescent probe BCECF with co-transfection of the trans-gene marker pEGFP-N1 (Life Technologies). We recorded BCECF fluorescence at the excitation wavelengths of 490 and 440 nm at a resolution of 2/s by using a recording setup (Delta Ram; PTI). Removal of  $\text{Cl}^-$  from the bath solution induced intracellular accumulation of  $\text{HCO}_3^-$  (increase in  $\text{pH}_i$ ) as a result of endogenous  $\text{Cl}_i\text{-HCO}_3^-_o$  exchange activities. Then, addition of 25 mM  $\text{SO}_4^{2-}$  to the bath solution evoked a reduction in  $\text{pH}_i$  as a result of  $\text{HCO}_3^-_i\text{-SO}_4^{2-}_o$  exchange activities. All experiments were performed at 37°C. (A–E) Representative traces of HEK293T cells expressing EGFP alone (A) and WT (B), p.Ala56Thr (C), p.Thr190Met (D), and p.Ser363Leu (E) SLC26A1 proteins. (F) Summaries of  $\text{HCO}_3^-$ -sulfate exchange activity. The intrinsic buffer capacity of HEK293T cells was 10.05 mM per pH unit (at  $\text{pH}_i$  7.0), and this value was not significantly different for cells transfected with WT or variant Slc26a1. Therefore, the  $\text{HCO}_3^-$ - $\text{SO}_4^{2-}$  exchange activities were presented as  $\Delta\text{pH}$  unit per min without compensating for the buffer capacity. Data are presented as mean  $\pm$  SEM. \* $p < 0.05$ , \*\* $p < 0.01$ .

hepatotoxicity. According to the findings in *Slc26a1*<sup>-/-</sup> mice, acetaminophen might be contraindicated in individuals with *SLC26A1* mutations.

### Supplemental Data

Supplemental Data include three figures and two tables and can be found with this article online at <http://dx.doi.org/10.1016/j.ajhg.2016.03.026>.

### Acknowledgments

We thank the physicians and the participating families for their contributions. We also thank Catherine Matero, Elizabeth Andrews, Brittany Fisher, Leslie Spaneas, and Jennifer Drucker for their help with patient enrollment and clinical information. F.H. is the Warren E. Grupe Professor of Pediatrics. This research was supported by grants DK1069274, DK1068306, and DK064614 (to F.H.) from the NIH, 6-FY11-241 (to F.H.) from the March of Dimes Foundation, 2013R1A3A2042197 (to M.G.L.) and 2015R1D1A1A01056685 (to H. Y. G) from the National Research

Foundation of Korea, Ministry of Science, ICT and Future Planning, and 2015-32-0047 (to H.Y.G) from the Yonsei University College of Medicine.

Received: February 15, 2016

Accepted: March 25, 2016

Published: May 19, 2016

### Web Resources

dbSNP, <http://www.ncbi.nlm.nih.gov/projects/SNP/>  
 Ensembl Genome Browser, <http://www.ensembl.org/index.html>  
 ExAC Browser, <http://exac.broadinstitute.org/>  
 GenBank, <http://www.ncbi.nlm.nih.gov/genbank/>  
 MutationTaster, <http://www.mutationtaster.org/>  
 NHLBI Exome Sequencing Project (ESP) Exome Variant Server, <http://evs.gs.washington.edu/EVS/>  
 OMIM, <http://www.omim.org/>  
 PolyPhen-2, <http://genetics.bwh.harvard.edu/pph2/>  
 RefSeq, <http://www.ncbi.nlm.nih.gov/RefSeq>  
 UCSC Genome Browser, <http://genome.ucsc.edu>

## References

1. Scales, C.D., Jr, Smith, A.C., Hanley, J.M., and Saigal, C.S.; Urologic Diseases in America Project (2012). Prevalence of kidney stones in the United States. *Eur. Urol.* *62*, 160–165.
2. Dwyer, M.E., Krambeck, A.E., Bergstralh, E.J., Milliner, D.S., Lieske, J.C., and Rule, A.D. (2012). Temporal trends in incidence of kidney stones among children: a 25-year population based study. *J. Urol.* *188*, 247–252.
3. Lotan, Y. (2009). Economics and cost of care of stone disease. *Adv. Chronic Kidney Dis.* *16*, 5–10.
4. Sayer, J.A. (2008). The genetics of nephrolithiasis. *Nephron, Exp. Nephrol.* *110*, e37–e43.
5. Edvardsson, V.O., Goldfarb, D.S., Lieske, J.C., Beara-Lasic, L., Anglani, F., Milliner, D.S., and Palsson, R. (2013). Hereditary causes of kidney stones and chronic kidney disease. *Pediatr. Nephrol.* *28*, 1923–1942.
6. Halbritter, J., Baum, M., Hynes, A.M., Rice, S.J., Thwaites, D.T., Gucev, Z.S., Fisher, B., Spaneas, L., Porath, J.D., Braun, D.A., et al. (2015). Fourteen monogenic genes account for 15% of nephrolithiasis/nephrocalcinosis. *J. Am. Soc. Nephrol.* *26*, 543–551.
7. Braun, D.A., Lawson, J.A., Gee, H.Y., Halbritter, J., Shril, S., Tan, W., Stein, D., Wassner, A.J., Ferguson, M.A., Gucev, Z., et al. (2016). Prevalence of Monogenic Causes in Pediatric Patients with Nephrolithiasis or Nephrocalcinosis. *Clin. J. Am. Soc. Nephrol.* *11*, 664–672.
8. Hunter, D.J., Lange, M., Snieder, H., MacGregor, A.J., Swaminathan, R., Thakker, R.V., and Spector, T.D. (2002). Genetic contribution to renal function and electrolyte balance: a twin study. *Clin. Sci. (Lond)* *103*, 259–265.
9. Goldfarb, D.S., Fischer, M.E., Keich, Y., and Goldberg, J. (2005). A twin study of genetic and dietary influences on nephrolithiasis: a report from the Vietnam Era Twin (VET) Registry. *Kidney Int.* *67*, 1053–1061.
10. Halbritter, J., Diaz, K., Chaki, M., Porath, J.D., Tarrier, B., Fu, C., Innis, J.L., Allen, S.J., Lyons, R.H., Stefanidis, C.J., et al. (2012). High-throughput mutation analysis in patients with a nephronophthisis-associated ciliopathy applying multiplexed barcoded array-based PCR amplification and next-generation sequencing. *J. Med. Genet.* *49*, 756–767.
11. Bissig, M., Hagenbuch, B., Stieger, B., Koller, T., and Meier, P.J. (1994). Functional expression cloning of the canalicular sulfate transport system of rat hepatocytes. *J. Biol. Chem.* *269*, 3017–3021.
12. Krick, W., Schnedler, N., Burckhardt, G., and Burckhardt, B.C. (2009). Ability of sat-1 to transport sulfate, bicarbonate, or oxalate under physiological conditions. *Am. J. Physiol. Renal Physiol.* *297*, F145–F154.
13. Xie, Q., Welch, R., Mercado, A., Romero, M.F., and Mount, D.B. (2002). Molecular characterization of the murine Slc26a6 anion exchanger: functional comparison with Slc26a1. *Am. J. Physiol. Renal Physiol.* *283*, F826–F838.
14. Dawson, P.A., Russell, C.S., Lee, S., McLeay, S.C., van Dongen, J.M., Cowley, D.M., Clarke, L.A., and Markovich, D. (2010). Urolithiasis and hepatotoxicity are linked to the anion transporter Sat1 in mice. *J. Clin. Invest.* *120*, 706–712.
15. Dawson, P.A., Sim, P., Mudge, D.W., and Cowley, D. (2013). Human SLC26A1 gene variants: a pilot study. *ScientificWorldJournal* *2013*, 541710.
16. Karniski, L.P., Lötscher, M., Fucntese, M., Hilfiker, H., Biber, J., and Murer, H. (1998). Immunolocalization of sat-1 sulfate/oxalate/bicarbonate anion exchanger in the rat kidney. *Am. J. Physiol.* *275*, F79–F87.
17. Quondamatteo, F., Krick, W., Hagos, Y., Krüger, M.H., Neubaue-Saile, K., Herken, R., Ramadori, G., Burckhardt, G., and Burckhardt, B.C. (2006). Localization of the sulfate/anion exchanger in the rat liver. *Am. J. Physiol. Gastrointest. Liver Physiol.* *290*, G1075–G1081.
18. Park, H.W., Nam, J.H., Kim, J.Y., Namkung, W., Yoon, J.S., Lee, J.S., Kim, K.S., Venglovecz, V., Gray, M.A., Kim, K.H., and Lee, M.G. (2010). Dynamic regulation of CFTR bicarbonate permeability by [Cl<sup>-</sup>]<sub>i</sub> and its role in pancreatic bicarbonate secretion. *Gastroenterology* *139*, 620–631.
19. Lee, A., Beck, L., and Markovich, D. (2003). The mouse sulfate anion transporter gene Sat1 (Slc26a1): cloning, tissue distribution, gene structure, functional characterization, and transcriptional regulation thyroid hormone. *DNA Cell Biol.* *22*, 19–31.
20. Markovich, D. (2012). Slc13a1 and Slc26a1 KO models reveal physiological roles of anion transporters. *Physiology (Bethesda)* *27*, 7–14.